Analysis of the pH Dependence of the Neonatal Fc Receptor/Immunoglobulin G Interaction Using Antibody and Receptor Variants†

Malini Raghavan,‡ Vincent R. Bonagura,§ Sherie L. Morrison,|| and Pamela J. Bjorkman*,‡,⊥

Division of Biology 156-29 and Howard Hughes Medical Institute, California Institute of Technology, Pasadena, California 91125, Long Island Jewish Medical Center, New Hyde Park, New York 11040, and Department of Microbiology and Molecular Genetics, University of California, Los Angeles, Los Angeles, California 90024

Received July 7, 1995; Revised Manuscript Received September 5, 1995⊗

ABSTRACT: The neonatal Fc receptor (FcRn) binds maternal immunoglobulin G (IgG) from ingested milk in the gut (pH 6.0−6.5) and delivers it to the bloodstream of the newborn (pH 7.0−7.5). A soluble version of FcRn reproduces the physiological pH-dependent interaction with IgG, showing high-affinity binding at pH 6.0−6.5 but weak or no binding at pH 7.0−7.5. We have studied the pH dependence of the FcRn/IgG interaction using a surface plasmon resonance assay to measure kinetic and equilibrium constants. We show that the affinity of FcRn for IgG is reduced about 2 orders of magnitude as the pH is raised from 6.0 to 7.0. A Hill plot analysis suggests that several titrating residues participate in the pH-dependent affinity transition. Histidine side chains are likely candidates for residues that titrate between pH 6.0 and 7.0, and previous biochemical and structural work identified several histidines on the Fc portion of IgG that are located at the FcRn binding site. Using mutant IgG molecules and IgG subtype variants that differ in the number of histidines at the IgG/FcRn interface, we demonstrate that IgG histidines located at the junction between the C_H2 and C_H3 domains (residues 310 and 433) contribute to the pH-dependent affinity transition. Experiments with a mutant FcRn molecule show that two histidines on the FcRn heavy chain (residues 250 and 251) also contribute to the pH dependence of the FcRn/IgG interaction. These results are interpreted using the crystal structures of FcRn and an FcRn/Fc complex.

Uptake of maternal immunoglobulin by the neonatal Fc receptor (FcRn)[1] expressed in the gut of newborn mammals allows the neonate to passively acquire humoral immunity against antigens encountered by the mother (Jones & Waldman, 1972). FcRn, expressed on the luminal side of intestinal epithelial cells, binds the Fc portion of maternal immunoglobulin G (IgG) from ingested milk (Rodewald & Kraehenbuhl, 1984). In a process called transcytosis, IgG molecules are transported across the gut epithelium to enter the bloodstream of the neonate. Transcytosis involves the internalization of FcRn/IgG complexes in clathrin-coated pits on the luminal side of intestinal epithelial cells, transit across the cell via uncoated vesicles and tubules, and delivery to the basolateral surface, where IgG dissociates into the blood (Rodewald & Kraehenbuhl, 1984). There is a net pH difference between the luminal surface (pH 6.0−6.5) and the basolateral surface (pH 7.4) of intestinal epithelial cells that facilitates the unidirectional transport of IgG (Rodewald, 1976). FcRn binds IgG at pH 6.0−6.5 but not at pH 7.4, suggesting that IgG dissociates from FcRn when exposed to the pH 7.4 environment of the blood and that the FcRn/IgG complexes are transported across the cell in acidic compartments (Rodewald & Kraehenbuhl, 1984).

FcRn was purified from intestinal brush borders on IgG affinity columns and shown to contain two subunits of molecular masses 45−50 and 14 kDa (Simister & Rees, 1985). Molecular cloning of the cDNA encoding the heavy chain of FcRn revealed the presence of three extracellular domains with sequence similarity to the α1, α2, and α3 domains of class I major histocompatibility (MHC) molecules, followed by a predicted transmembrane region and a short cytoplasmic tail (Simister & Mostov, 1989a,b). The 14 kDa subunit of FcRn was identified as β2-microglobulin (β2m) (Simister & Rees, 1985), the class I MHC light chain. FcRn expressed on the surface of transfected cells (Simister & Mostov, 1989a,b; Gastinel *et al.*, 1992) and purified soluble FcRn heterodimers (Gastinel *et al.*, 1992) bind IgG at pH 6.5 but not at pH 7.5, consistent with the binding properties of FcRn from neonatal rat intestine. By contrast, class I MHC molecules are not known to demonstrate a similar pH dependence in binding to their ligands, which are peptides, T cell receptors, and the T cell coreceptor CD8. The pH dependence of the FcRn/IgG interaction therefore appears to be an inherent property of the FcRn/IgG complex, presumably an evolutionary adaptation to ensure unidirectional transport of IgG from the gut to the blood.

† Supported by a Camille and Henry Dreyfuss Teacher Scholar Award (P.J.B.), the Howard Hughes Medical Institute (P.J.B.), a postdoctoral fellowship from the Cancer Research Institute (M.R.), and grants from the NIH (CA16858 and AI29470 to S.L.M.).

* To whom correspondence should be addressed.
‡ Division of Biology 156-29, California Institute of Technology.
§ Long Island Jewish Medical Center.
|| University of California, Los Angeles.
⊥ Howard Hughes Medical Institute, California Institute of Technology.

⊗ Abstract published in *Advance ACS Abstracts,* November 1, 1995.

[1] Abbreviations: BCA, bicinchoninic acid; β2m, β2-microglobulin; EDC, *N*-ethyl-*N*′-[3-(diethylamino)propyl]carbodiimide; FcRn, Fc receptor, neonatal; hIgG4, human immunoglobulin G 4; IgG, immunoglobulin G; K_A, equilibrium association constant; K_D, equilibrium dissociation constant; k_a, association rate constant; k_d, dissociation rate constant; mIgG2a, murine immunoglobulin G 2a; mIgG2b, murine immunoglobulin G 2b; MHC, major histocompatibility complex; NHS, *N*-hydroxysuccinimide; RU, resonance units; SPR, surface plasmon resonance.

0006-2960/95/0434-14649$09.00/0

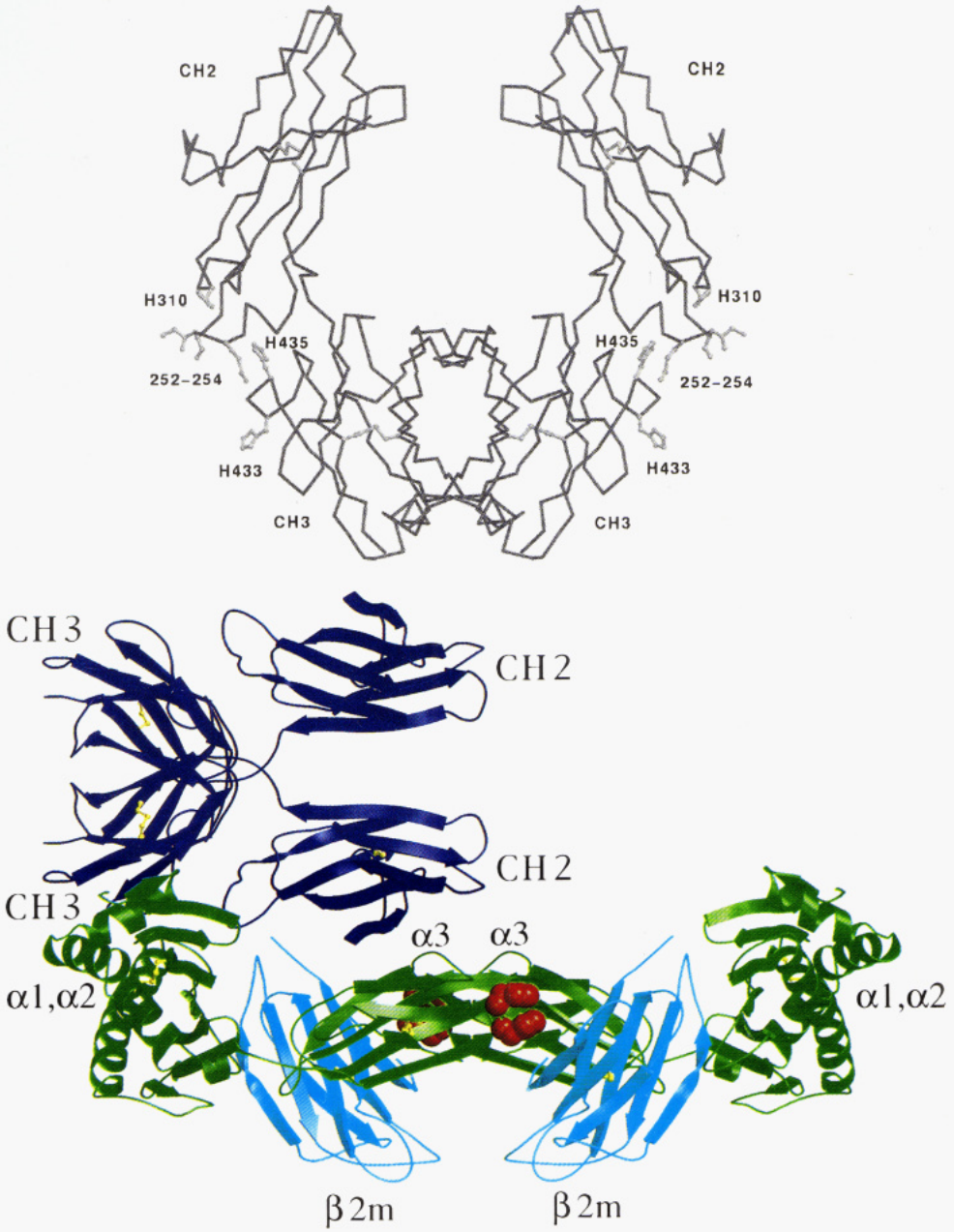

FIGURE 1: (A, top) Fc residues investigated in this study highlighted on a carbon-α representation of the structure of human Fc (Deisenhofer, 1981). (B, bottom) Ribbon diagram representation of the FcRn dimer (heavy chain, green; β2m domain, light blue) that interacts with a single Fc (dark blue), as observed in the crystal structure of the FcRn/Fc complex (Burmeister *et al.*, 1994a). FcRn histidines 250 and 251 are highlighted in red on each heavy chain. These figures were generated using MOLSCRIPT (Kraulis, 1991).

In order to quantify the magnitude of the affinity change in FcRn/IgG complexes as a function of pH, we used a surface plasmon resonance (SPR) assay (Fägerstam *et al.*, 1992; Malmqvist, 1993). We find that the affinity of FcRn/IgG complexes is exquisitely sensitive to pH, being reduced by over 2 orders of magnitude as the pH is raised from 6.0 to 7.0. The mechanistic basis of the affinity transition is of interest since such a sharply pH-dependent interaction is unusual for protein/protein interactions. Because imidazole side chains of histidine residues usually deprotonate over the pH range 6.0−7.0, the pH dependence of the FcRn/IgG interaction was suggested to involve histidines either directly at the interaction site (Simister & Mostov, 1989b) or indirectly by causing a structural change in FcRn that facilitates IgG release at basic pH (Raghavan *et al.*, 1993).

The finding that fragment B of protein A inhibits FcRn binding to IgG (Raghavan *et al.*, 1994) suggested that the FcRn binding site on Fc is the interface between the C_H2-C_H3 domains, the fragment B binding site deduced from crystallographic studies (Deisenhofer, 1981). Three nearly conserved histidines (Fc residues 310, 433, and 435; Figure 1A) at the fragment B binding interface were suggested to be responsible for the pH-dependent interaction between FcRn and IgG (Raghavan *et al.*, 1994). The solution of a low-resolution FcRn/Fc cocrystal structure (Burmeister *et al.*, 1994a) (Figure 1B) confirmed that FcRn contacts Fc at the C_H2-C_H3 domain interface and showed probable contacts between FcRn and Fc histidines 310, 433, and 435. Fc residues 310 and 433 were further implicated as important for FcRn function in recent studies using mutant Fc fragments that were defective in transcytosis from the gut into the serum and in binding to brush border membranes of neonatal mice (Kim *et al.*, 1994a). In order to directly evaluate the contribution of the Fc histidines at the FcRn binding site in

the pH-dependent affinity transition, we measured binding affinities and evaluated the pH dependence of IgG variants with alterations of histidines 310, 433, and 435. These residues are nearly completely conserved in human, mouse, and rat IgG subtypes (Kabat *et al.*, 1991). One exception is murine IgG2b (mIgG2b), in which residue 433 is a lysine and residue 435 is a tyrosine. The participation of one or both of these residues in the pH-dependent affinity transition is confirmed by our observations that the pH-dependent affinity transition is less sharp for mIgG2b than for murine IgG2a (mIgG2a) and that there is a reduction in the pH dependence of the dissociation rate for mIgG2b compared to mIgG2a. Using previously described chimeric human IgG4 (hIgG4) molecules with mutations in the Fc region (Artandi *et al.*, 1992), we further demonstrate that alteration of residues 309−311, but not residue 435, affects the FcRn/IgG interaction, thereby implicating histidine 310 but not histidine 435.

We previously identified two histidine residues on the FcRn heavy chain (residues 250 and 251; Figure 1B) that affect the binding affinity for IgG at pH 6.0 (Raghavan et al., 1994). In the present study, we show that mutation of these FcRn histidines results in a reduction in the pH dependence of the dissociation rate of IgG, similar to the results observed for the IgG variants and mutants. Taken together, the results reported in this paper demonstrate the involvement of residues 310 and 433 of the Fc portion of IgG, and residues 250 and/or 251 of FcRn, in effecting a pH-dependent reduction in the binding affinity of FcRn for IgG at pH 7.0 and above.

MATERIALS AND METHODS

Reagents. Monoclonal mIgG2a and mIgG2b (specific for the hapten trinitrophenol) were purchased from Pharmingen. Results presented for mIgG2a were verified using an anti-dansyl mIgG2a (Pharmingen) and the anti-HLA-B27 monoclonal antibody B27M1 (American Tissue Culture Collection). Results presented for mIgG2b were verified using an anti-dansyl mIgG2b (Pharmingen) and monoclonal mIgG2b's from Cappel and Zymed. *N*-Ethyl-*N'*-(3-diethylaminopropyl)carbodiimide (EDC), *N*-hydroxysuccinimide (NHS), ethanolamine, BIAcore surfactant P20, and certified CM5 sensor chips were obtained from Pharmacia Biosensor. Bicinchoninic acid (BCA) assay reagents were from Pierce.

Expression of hIgG4 and Derived Mutants. The expression of hIgG4 molecules and derived mutants was described previously (Artandi *et al.*, 1992). These chimeric molecules are composed of a murine anti-dansyl V_H domain fused to the constant domains (C_H1 through C_H3) of human IgG4. An expression vector containing DNA encoding the hybrid heavy chain was cotransfected into a non-Ig-producing mouse myeloma cell line along with an expression vector containing DNA encoding a chimeric κ light chain (composed of a murine anti-dansyl Vκ region fused to the human Cκ region). Site-directed mutations were introduced into the chimeric heavy chain gene to make the following mutants (Artandi *et al.*, 1992): H435R, in which histidine 435 was changed to an arginine; 309−311 in which residues 309−311 were changed from the sequence LHQ to the sequence GGG; and 252−254 in which residues 252−254 were changed from the sequence MIS to GGG.

Expression of FcRn Mutant H250Q-H251N. The construction and expression of lipid-linked forms of mutant and wild-type rat FcRn heterodimers in Chinese hamster ovary cells were previously described (Raghavan *et al.*, 1994; Gastinel *et al.*, 1992). FcRn mutant H250Q-H251N is a heterodimer in which mutations were introduced to change His 250 to glutamine and His 251 to asparagine in a truncated rat FcRn heavy chain (residues 1−269) which is paired with a lipid-linked version of rat β2m (Raghavan *et al.*, 1994). The wild-type FcRn used for comparisons with this mutant FcRn molecule consists of the counterpart truncated wild-type FcRn heavy chain also paired with lipid-linked rat β2m.

Protein Purification. Secreted FcRn (a heterodimer composed of residues 1−269 of the rat FcRn heavy chain associated with rat β2m) was purified from supernatants of transfected Chinese hamster ovary cells using pH-dependent binding to rat IgG affinity columns (Gastinel *et al.*, 1992). Soluble versions of the lipid-linked wild-type and H250Q-H251N mutant FcRn molecules were purified similarly after release of the proteins from the membranes of transfected cells with phosphatidylinositol-specific phospholipase C (Raghavan *et al.*, 1994). M1/42 (rat IgG2a) was purified using immobilized FcRn (Huber *et al.*, 1993). The chimeric hIgG4 protein and derived mutants were purified from cell supernatants as previously described (Tao & Morrison, 1989). FcRn and IgG concentrations were estimated using BCA assays with bovine serum albumin as the standard.

Immobilization of IgG and FcRn on Biosensor Chips. A BIAcore biosensor system (Pharmacia LKB Biotechnology, Inc.) was used for real time binding experiments. This system includes a biosensor element with a dextran-coated gold surface to which FcRn or IgG was coupled using standard amine coupling chemistry as described in the BIAcore manual. Immobilization of secreted wild-type FcRn (for experiments with IgG mutants and variants) was accomplished by initial activation of the sensor chip with 0.05 M NHS and 0.2 M EDC, followed by reaction with 0.5 mg/mL FcRn equilibrated in 10 mM citrate, pH 4.0. Immobilization of M1/42 rat IgG using amine coupling chemistry (for experiments with the H250Q-H251N FcRn mutant) was previously described (Raghavan *et al.*, 1994). Any remaining unreacted NHS ester groups were blocked by 1 M ethanolamine, pH 8.5.

Determination of K_D Values of FcRn/IgG Complexes by BIAcore Analysis. Binding of IgG or FcRn to the protein immobilized on the biosensor chip results in changes in the SPR signal that are directly proportional to the amount of bound protein and read out in real time as resonance units (RU) (Fägerstam *et al.*, 1992; Malmqvist, 1993). Kinetic and equilibrium constants were derived by analysis of plots of RU versus time (sensorgrams). The affinities of mIgG2a and mIgG2b for FcRn were calculated at pH values between 6.0 and 7.0 by analysis of data obtained from injections at each pH value of different concentrations of IgG samples in 50 mM phosphate and 150 mM NaCl. Each injection onto an FcRn-coupled flow cell was followed by an identical injection onto a blank flow cell of the same chip in order to subtract out nonspecific responses. Accurate kinetic measurements at high pH values are not possible because the dissociation rates are very rapid, and rapid association kinetics result from the high protein concentrations required to observe binding. Affinities were therefore estimated at each pH value by Scatchard analysis, using a plot (data not shown) of R_{eq}/C versus R_{eq} (R_{eq} is the net equilibrium response [$R_{\text{FcRn flow cell}} - R_{\text{blank flow cell}}$]; C is the IgG concentra-

tion). At low pH values, the Scatchard plots are biphasic over the concentration range used, but only data points corrresponding to the high-affinity population were taken into account for calculations of the affinity constant.

To measure K_D values for the interaction of FcRn with chimeric hIgG4 or its mutants, different concentrations of wild-type or mutant hIgG4 were injected over the FcRn-coupled biosensor chip. High-affinity binding constants were calculated from estimates of the kinetic association and dissociation rate constants rather than Scatchard analyses, since the binding of the 309−311 and the 252−254 mutants to FcRn does not approach equilibrium within the time frame of the BIAcore experiments. Although a detailed analysis of the binding curves shows the existence of populations of FcRn with high and low affinity for IgG, the high-affinity population predominates (>80%) over the IgG concentration ranges used in these experiments. Binding constants were therefore estimated assuming single averaged rate constants for the association and dissociation phases and are thus representative of the high-affinity population.

Analysis of the pH Dependence of Dissociation Rates. IgG or FcRn samples were bound at pH 6.0 to a biosensor chip to which the partner molecule had been immobilized. Buffers (50 mM sodium phosphate, 150 mM NaCl) were injected at pH values from 6.0 to 7.0 after the complexes had been allowed to dissociate for 1 min at pH 6.0. As the pH of the buffer is raised from 6.0 to 7.0, the net dissociation rate of the FcRn/IgG complexes increases since the affinity is reduced. The BIAevaluation 2.0 software package was used to fit the dissociation curves using a single exponential dissociation rate equation ($y = Re^{-k_d t}$, where R is the observed response at the start of the dissociation and k_d is the dissociation rate constant) or a biexponential dissociation rate equation ($y = R_{fast}e^{-k_{d\,fast}t} + R_{slow}\,e^{-k_{d\,slow}t}$, where $k_{d\,slow}$ and $k_{d\,fast}$ represent fast and slow dissociation rate constants and R_{slow} and R_{fast} correspond to the fraction of complexes dissociating with each rate constant). Using the BIAevaluation 2.0 software, an F-test-based comparison between derived chi-squared values for the single exponential or biexponential fits yielded an estimated probability for each dissociation curve of which model produced the best fit to the data. In all cases for which two k_d values are reported, the probability that the biexponential model is valid was greater than 0.99. Using the derived % R values and/or rate constants, $t_{1/2}$ values were calculated at each pH by solving the single exponential or biexponential rate equation for $y = 0.5$ using Mathematica (Wolfram, 1991).

RESULTS

The Affinity of FcRn for IgG Is Sharply Reduced As the pH Is Raised from 6.0 to 7.0. We were interested in quantitating the pH dependence of the affinities of FcRn/IgG complexes and particularly in comparing the affinity variation as a function of pH for mIgG2b compared to other IgGs, since mIgG2b lacks two of the conserved histidines at the FcRn binding interface. The crystal structure of an FcRn/Fc complex (Burmeister *et al.*, 1994a) suggests that the most notable changes at the FcRn binding interface of mIgG2b compared to mIgG2a are the substitution of histidines 433 and 435 (mIgG2a) for lysine and tyrosine (mIgG2b). Table 1A compares the variation of the high-affinity binding constants as a function of pH for complexes of FcRn with mIgG2a and mIgG2b. The binding constant of the FcRn/mIgG2a complex is reduced by over 100-fold as the pH is raised from 6.0 to 7.0 (100-fold is a lower

Table 1: Comparison of the pH Dependence of Affinity and Kinetic Constants for FcRn Binding to mIgG2a and mIgG2b[a]

(A) pH-Dependent Variation of Equilibrium Constants

	K_D (nM)			
pH	mIgG2a	mIgG2b	mIgG2a	mIgG2b
6.00	311	242	137	195
6.20			210	260
6.40			368	763
6.60			1270	1388
6.75			3900	2356
6.90			6900	4558
7.00	>30000	14600		
K_D(high pH)/K_D(low pH)	>100	60	50	23

(B) pH-Dependent Variation of Dissociation Rate Constants

pH	$k_{d\,slow}$ ($s^{-1} \times 10^{-3}$)	$k_{d\,fast}$ ($s^{-1} \times 10^{-3}$)	R_{slow} (%)	R_{fast} (%)	$t_{1/2}$ (min)
mIgG2a					
6.00	1.24		100	0	9.3
6.25	1.83	13.7	83.1	16.9	4.7
6.50	3.60	23.0	69.2	31.8	1.8
6.75	7.83	43.0	59.2	40.9	0.7
7.00	11.50	60.5	33.9	66.1	0.3
	$t_{1/2}$(pH 6.0)/$t_{1/2}$(pH 7.0) = 31.0				
mIgG2b					
6.00	1.56	11.3	96.6	3.4	7.0
6.25	1.75	26.4	89.2	10.8	5.5
6.50	2.73	24.7	76.5	23.5	2.7
6.75	3.50	39.2	71.0	29.0	1.7
7.00	3.50	46.4	58.2	41.8	1.0
	$t_{1/2}$(pH 6.0)/$t_{1/2}$(pH 7.0) = 7.0				

[a] For all experiments, FcRn was immobilized on a biosensor chip to a final response between 2000 and 2500 RU. (Part A) Variation of K_D with pH for binding of anti-trinitrophenol mIgG2a and anti-trinitrophenol mIgG2b to FcRn. K_D values for high-affinity binding constants are derived as described in Materials and Methods from biosensor assays in which different concentrations of each IgG sample were injected at the specified pH values over FcRn immobilized onto a biosensor chip. The two sets of K_D values listed for each mIgG (measurements at pH 6.0 and 7.0 and measurements between pH 6.0 and 6.9) correspond to results obtained from independent experiments that were performed on different FcRn-coupled chips. At pH 7.0, there is no specific binding observed at mIgG2a concentrations below 30 μM, suggesting a K_D of 30 μM or weaker. (Part B) Comparison of the pH dependence of the dissociation rates of anti-trinitrophenol mIgG2a/FcRn and anti-trinitrophenol mIgG2b/FcRn complexes. At approximately 1 min into the dissociation phase, buffers (50 mM sodium phosphate, 150 mM NaCl) were injected at pH values from 6.0 to 7.0. % R values and/or rate constants were calculated at each pH value by nonlinear analysis of the dissociation curves assuming a single exponential or biexponential dissociation rate equation. Using the derived % R values and/or rate constants, $t_{1/2}$ values were calculated at each pH by solving the biexponential rate equation for $y = 0.5$ using Mathematica (Wolfram, 1991). To verify the results using anti-trinitrophenol mIgG's, the measurements were repeated using different commercial preparations of mIgG2a and mIgG2b. The average $t_{1/2}$(low pH)/$t_{1/2}$(high pH) ratio for three independent experiments using the anti-trinitrophenol mIgG2a was 39.3, compared to a ratio of 12.9 for the anti-dansyl mIgG2a and 14.9 for the B27M1 mIgG2a. The average $t_{1/2}$(low pH)/$t_{1/2}$(high pH) ratio for three independent experiments using the anti-dansyl mIgG2b was 4.1, compared to a ratio of 7.3 for an mIgG2b from Zymed and 1.9 for an mIgG2b from Kappel. The reason for the variability is unknown but could reflect uncharacterized sequence differences in the Fc regions of different murine antibodies assumed to be the same subtype. Importantly, all of the mIgG2b proteins examined showed less pH dependence than the mIgG2a proteins that were studied.

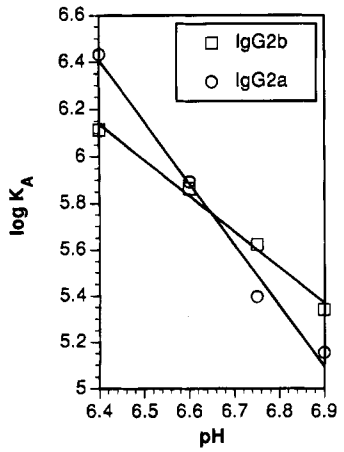

FIGURE 2: Comparative Hill plots (log K_A versus pH) for the FcRn/mIgG2a interaction (open circles) and the FcRn/mIgG2b interaction (open squares). K_A values were determined from a Scatchard analysis using BIAcore data as described in Materials and Methods. Only K_A values at pH 6.4 and above were used for the Hill analysis, since the K_A remains relatively constant at pH values below 6.4. The slope of each plot (the Hill coefficient) is indicative of the number of residues that deprotonate and participate in the affinity change. For anti-trinitrophenol mIgG2a, the derived slope is −2.6 (suggesting the involvement of three titrating residues), compared to −1.6 for anti-trinitrophenol mIgG2b (suggesting the involvement of two titrating residues). The affinity between IgG and FcRn becomes even weaker above pH 6.9, but affinities at pH values above 6.9 are difficult to measure because of the weakness of the FcRn/IgG interaction at neutral or basic pH. It is therefore possible that more than three and two titrating residues are involved in the overall affinity transitions for the interactions of mIgG2a and mIgG2b with FcRn.

estimate of the affinity reduction since an accurate measurement of the affinity at pH 7.0 was not possible due to the weakness of the interaction). We observe a similar reduction (>100-fold) in the affinity of FcRn for rat IgG2a over the pH range 6.0−7.1 (data not shown) and expect the same trend with other human, mouse, and rat IgG subtypes, all of which show pH-dependent binding to FcRn (Wallace & Rees, 1980) and almost complete conservation of histidines at positions 310, 433, and 435 (Kabat *et al.*, 1991). In contrast to the FcRn interaction with mIgG2a and rat IgG2a, the pH dependence of the binding of mIgG2b to FcRn is not as pronounced. FcRn shows a weak but measurable binding affinity for mIgG2b at pH 7.0 and an overall reduction in affinity of only 60-fold as the pH is raised from 6.0 to 7.0.

To obtain an estimate of the number of residues that deprotonate and participate in the pH-dependent affinity change, we performed a series of affinity measurements for FcRn/mIgG2a and FcRn/mIgG2b complexes at six different pH values between 6.0 and 6.9. The slope derived from a plot of log K_A (the equilibrium association constant) versus pH (a Hill plot) is indicative of the number of titrating residues over a given pH range. Figure 2 shows Hill plots for the pH dependence of the affinities of FcRn for mIgG2a compared to mIgG2b over the pH range where the affinity change is most pronounced (pH 6.4−6.9). For mIgG2a, the derived slope is −2.6, compared to a slope of −1.6 for mIgG2b. Approximating the slopes derived for mIgG2a and mIgG2b to −3 and −2, respectively, these data suggest that three residues on the mIgG2a/FcRn complex and two residues on the mIgG2b/FcRn complex titrate over the pH range from 6.4 to 6.9 to effect the pH-dependent affinity transition. These results suggest that one or more of the absent histidines on mIgG2b account, at least in part, for the pH dependence of FcRn interactions with other IgG subtypes.

Comparison of the Dissociation Rates of FcRn/mIgG2a and FcRn/mIgG2b Complexes. In order to estimate the physiological lifetimes of FcRn/IgG complexes upon exposure to the neutral or slightly basic pH environment at the basolateral surface of intestinal epithelial cells, we studied the pH dependence of the dissociation rates of IgG/FcRn complexes. Complexes of FcRn with mIgG2a or mIgG2b were formed at pH 6.0 by passing solutions of each IgG over a biosensor chip to which FcRn was immobilized. Approximately 1 min after the end of the IgG injection, buffers were injected at various pH values from 6.0 to 7.0. Dissociation rates at each pH value were estimated by nonlinear analysis of the dissociation curves using a single exponential or biexponential rate equation to fit the dissociation curves. Table 1B shows the variation as a function of pH of the derived rate constants ($k_{d\,slow}$, representative of a higher affinity FcRn/IgG population, and $k_{d\,fast}$, representative of a lower affinity FcRn/IgG population), the percentages of the total population with each rate constant (R_{slow} and R_{fast}), and the time required for half of the complexes to dissociate ($t_{1/2}$). As expected, the time it takes for half of the complexes to dissociate decreases as the pH is raised from 6.0 to 7.0. However, the $t_{1/2}$ values for mIgG2a/FcRn complexes show a greater drop with increasing pH than the $t_{1/2}$ values for mIgG2b/FcRn complexes, thereby demonstrating that the dissociation rate of mIgG2b from FcRn has a reduced pH dependence compared to the dissociation rate of mIgG2a. Since the $t_{1/2}$ values are calculated from the derived rate constants and % R values, the differences in $t_{1/2}$ values for the two mIgG subtypes are a combination of two effects: (1) At pH 7.0, the slow and fast rate constants derived for mIgG2a are faster than the rate constants derived for mIgG2b. (2) At pH 7.0, fewer FcRn/mIgG2b complexes compared to FcRn/mIgG2a complexes dissociate with the fast rate constant (compare R_{fast} for mIgG2b versus mIgG2a).

These results indicate that FcRn/mIgG2b complexes formed at low pH have a longer lifetime upon exposure to a pH 7.0 environment than FcRn/mIgG2a complexes, again suggesting that one or both of the absent histidines on mIgG2b account in part for the pH dependence of the dissociation rates of FcRn complexes with other IgG's.

IgG Residues 309−311 and 252−254 of IgG Are Involved in FcRn Binding. The binding site on IgG for rheumatoid factor (RF) autoantibodies has been localized to the interface between the C_H2 and the C_H3 domains (Artandi *et al.*, 1992). Residues 435, 309−311, and 252−254 of IgG were identified as part of the binding site using chimeric hIgG4 mutants in which these residues were altered (residue 435 was changed from His to Arg, residues 309−311 were changed from the sequence LHQ to the sequence GGG, and residues 252−254 were changed from the sequence MIS to the sequence GGG) (Artandi *et al.*, 1992). We analyzed the binding affinities of these IgG mutants for FcRn since the IgG residues that were altered are also predicted to form part of the FcRn binding interface, based upon the FcRn/Fc cocrystal structure (Burmeister *et al.*, 1994a). The hIgG4 and derived mutant proteins were not available in sufficent quantities to allow a full analysis of the pH-dependent affinity transition for binding to FcRn; therefore the affinities of each protein

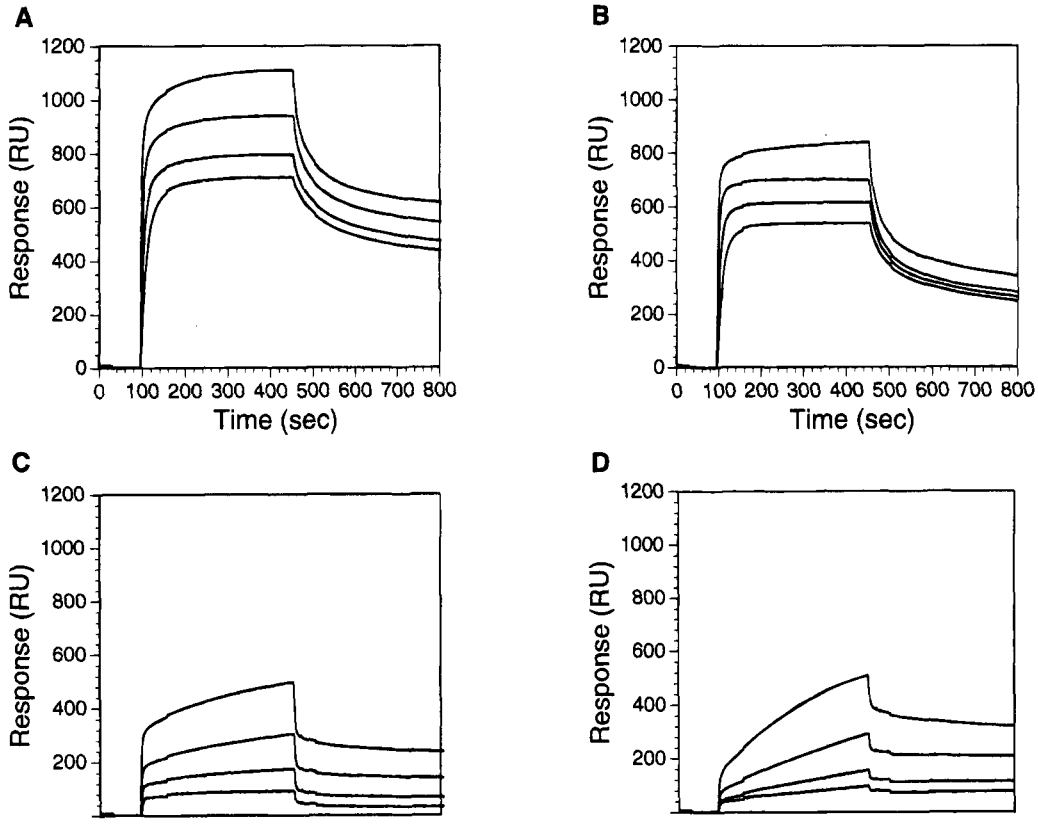

FIGURE 3: Sensorgrams from SPR assays of the interaction of FcRn with hIgG4 and derived mutants. FcRn was coupled to a biosensor chip to 2250 RU using amine coupling chemistry. Multiple injections corresponding to different concentrations of each IgG were performed as specified below. Sensor chip surfaces were regenerated between different injections by injecting 50 mM phosphate and 150 mM NaCl, pH 7.5. (A) Injection of wild-type hIgG4 at concentrations of 229, 460, 920, or 1840 nM. (B) Injection of the H435R mutant at concentrations of 208, 416, 832, or 1664 nM. (C) Injection of the 309−311 (LHQ to GGG) mutant at concentrations of 275, 550, 1100, or 2200 nM. (D) Injection of the 252−254 (MIS to GGG) mutant at concentrations of 208, 416, 832, or 1664 nM.

for FcRn were evaluated only at pH 6.0, and dissociation rates of the various complexes were analyzed as a function of pH (see below). Figure 3 shows sensorgrams for the binding to FcRn of the hIgG4 protein or a derived mutant. Visual inspection of the sensorgrams reveals that the binding of the 309−311 mutant (LHQ to GGG) and the 252−254 mutant (MIS to GGG) is impaired compared to the hIgG4. The effect of both sets of mutations is primarily upon the association phase of the binding (Figure 3, Table 2A). Table 2A shows the derived association and dissociation rate constants and the calculated binding constants, revealing that alteration of IgG residues 252−254 and 309−311 significantly affects the binding to FcRn. The reduced affinity resulting from both sets of mutations is predominantly due to a lower association rate constant. By contrast, the dissociation rate constants for both mutants are very similar to the rate constant obtained for the wild-type protein.

Comparison of the Dissociation Rates of FcRn/hIgG4 and FcRn/Mutant hIgG4 Complexes. hIgG4/FcRn and mutant hIgG4/FcRn complexes were assembled at pH 6.0 by flowing solutions of each IgG over an immobilized FcRn biosensor chip, and dissociation rates were calculated at various pH values as described for the mIgG analyses. Table 2B compares the pH-dependent dissociation from FcRn of hIgG4 and the 309−311 (LHQ to GGG) and H435R mutants. The pH dependence of the dissociation rate of the 252−254 mutant (MIS to GGG) was not examined since no residues expected to titrate in the pH 6.0−7.0 range were altered. The dissociation rate behavior of wild-type hIgG4/FcRn and H435R hIgG4/FcRn complexes as a function of pH is comparable, implying that histidine 435 is not involved in effecting enhanced dissociation of the FcRn/IgG complex at high pH. However, the dissociation rate of the 309−311 hIgG4/FcRn complex shows a reduction in pH dependence compared to wild-type hIgG4/FcRn and H435R/FcRn complexes, based upon the criteria used above to evaluate the pH dependence of mIgG2a and mIgG2b dissociation rates. These results imply that titration of histidine 310, but not histidine 435, can account in part for the pH dependence of the dissociation rates of FcRn/IgG complexes.

Comparison of the Dissociation Rates of Mutant FcRn/IgG and Wild-Type FcRn/IgG Complexes. Previous experiments demonstrated that alteration of FcRn histidines 250 and 251 affects the affinity for IgG (Raghavan *et al.*, 1994). BIAcore analysis of the interaction of the FcRn H250Q-H251N mutant and wild-type FcRn with IgG at pH 6.0 showed that the affinity of the mutant for IgG was reduced compared to wild type by 6−7-fold (Raghavan *et al.*, 1994). In order to ascertain if these FcRn histidine residues affect the pH dependence of the dissociation rate of FcRn/IgG complexes, we compared the dissociation rates of mutant and wild-type FcRn/IgG complexes as a function of pH. FcRn wild-type or H250Q-H251N mutant/IgG complexes were assembled at pH 6.0 by flowing solutions of each FcRn molecule over a biosensor chip to which the rat IgG2a antibody M1/42 had been immobilized. Dissociation rates were calculated at various pH values as described for the mIgG analyses. A difference is seen in the pH dependence of the dissociation rates of the wild-type and mutant FcRn molecules, with the pH dependence of the mutant being

Table 2: Comparison of the Affinity Constants and the pH Dependence of the Dissociation Rates for FcRn Binding to hIgG4 and Derived Mutants[a]

(A) Equilibrium Constant Measurements at pH 6.0

IgG	k_a (M^{-1} s^{-1} × 10^3)	k_d (s^{-1} × 10^{-3})	K_D (nM; pH 6.0)
hIgG4	188.5 ± 52.0	3.66 ± 0.12	21.5 ± 7.5
H435R	229.3 ± 65.7	4.95 ± 0.18	24.1 ± 8.7
309−311 (LHQ to GGG)	1.7 ± 0.3	2.90 ± 0.21	1713.5 ± 224.0
252−254 (MIS to GGG)	1.6 ± 0.5	2.79 ± 0.47	1878.0 ± 337.9

(B) pH-Dependent Variation of Dissociation Rate Constants

pH	$k_{d\ slow}$ (s^{-1} × 10^{-3})	$k_{d\ fast}$ (s^{-1} × 10^{-3})	R_{slow} (%)	R_{fast} (%)	$t_{1/2}$ (min)
hIgG4					
6.00	0.67		100.0	0	17.2
6.25	1.38		100.0	0	8.3
6.50	1.25	10.5	85.3	14.7	7.1
6.75	2.80	17.7	75.0	25.0	2.6
7.00	6.00	34.5	47.4	52.6	0.7
	$t_{1/2}$(pH 6.0)/$t_{1/2}$(pH 7.0) = 24.6				
H435R					
6.0	1.02		100.0	0	11.3
6.25	1.36	26.8	94.1	5.9	7.7
6.50	2.12	21.3	77.0	23.0	3.4
6.75	1.92	24.3	54.9	45.1	1.6
7.00	2.89	41.8	30.0	70.0	0.5
	$t_{1/2}$(pH 6.0)/$t_{1/2}$(pH 7.0) = 22.6				
309−311 (LHQ to GGG)					
6.00	0.92		100.0	0	12.5
6.25	1.83		100.0	0	6.3
6.75	2.56	20.9	83.9	16.1	3.4
7.00	3.45	24.9	67.1	32.9	1.7
	$t_{1/2}$(pH 6.0)/$t_{1/2}$(pH 7.0) = 7.3				

[a] For all experiments, FcRn was immobilized on a biosensor chip to a final response between 2250 and 2700 RU. (Part A) Affinity constants at pH 6.0. Chimeric hIgG4 or mutant hIgG4 samples were injected at concentrations between 200 nM and 7 μM. K_D values were calculated from the on- and off-rate constants derived for the sensorgrams shown in Figure 3 for hIgG4 and H435R. For the 309−311 and 252−254 mutants that showed a reduced affinity, the IgG concentration range used to evaluate the K_D values was 1.1−8.8 μM and 1.7−6.7 μM (affinity estimates at lower IgG concentrations were not possible because most of the observed response corresponded to nonspecific binding). (Part B) Comparison of the pH dependence of the dissociation rates of wild-type and mutant hIgG4/FcRn complexes. At approximately 1 min into the dissociation phase, buffers (50 mM sodium phosphate, 150 mM NaCl) were injected at pH values from 6.0 to 7.0. Rate constants, % R, and $t_{1/2}$ values were calculated as described in Materials and Methods and the legend to Table 1. The pH 6.0 k_d values derived in this part of the table are slower than the corresponding k_d values derived in part A because the rates reported in part A represent initial dissociation rates, rather than rates observed 1 min into the dissociation phase. Analysis of the dissociation curves using the BIAevaluation 2.0 software shows the existence of slow- and fast-dissociating components during the initial phase of the dissociation. For simplification of affinity constant calculations, the assumption of a single averaged rate constant was made for derivation of k_d values in part A.

reduced compared to the wild-type FcRn (Table 3).

DISCUSSION

Measurements of affinities of FcRn for IgG as a function of pH for different IgG species and subtypes reveal the exquisite sensitivity of FcRn/IgG complex formation to pH. The affinity of FcRn for IgG is reduced by over 2 orders of magnitude as the pH is raised from 6.0 to 7.0. At pH values between 5.5 and 6.0, we find much less variability in the dissociation rates and affinity constants of FcRn/IgG complexes. For example, at pH 5.7, the affinity of the FcRn/IgG complex is about 1.3-fold higher than the affinity at pH 6.0 (data not shown), suggesting that FcRn/IgG complexes are stable during transcytosis in vesicles in which pH values between 5.5 and 6.0 might be expected. *In vivo*, the sharply pH-dependent interaction between pH 6.0 and 7.0 ensures efficient unidirectional transport of IgG from the gut (pH 6.0−6.5) into the blood (pH 7.0−7.5). Since imidazole side chains of histidine residues usually deprotonate over the pH range from 6.0 to 7.0, the pH dependence of the FcRn/IgG interaction was suggested to involve histidines either directly at the interaction site (Simister & Mostov, 1989b) or indirectly by causing a conformation change in FcRn (Raghavan *et al.*, 1993). The experiments reported here were designed to assess the effects of IgG histidines 310, 433, and 435 that are located at the FcRn binding interface (Figure 1A) (Burmeister *et al.*, 1994a).

Table 3: Comparison of the pH Dependence of the Dissociation Rates of Wild-Type and Mutant FcRn/IgG Complexes[a]

pH-Dependent Variation of Dissociation Rate Constants

pH	$k_{d\ slow}$ (s^{-1} × 10^{-3})	$k_{d\ fast}$ (s^{-1} × 10^{-3})	R_{slow} (%)	R_{fast} (%)	$t_{1/2}$ (min)
wild-type FcRn					
6.00	1.63		100.0	0	7.1
6.50	5.38	26.9	80.7	19.3	1.6
6.75	12.80	45.9	68.8	31.2	0.6
7.00	23.00	70.0	38.2	61.8	0.15
	$t_{1/2}$(pH 6.0)/$t_{1/2}$(pH 7.0) = 47.3				
H250Q−H251N FcRn mutant					
6.00	0.19	8.4	32.4	67.5	2.6
6.25	6.99	20.0	69.8	31.2	1.2
6.50	3.65	24.0	28.9	71.1	0.7
6.75	14.20	64.0	41.5	58.5	0.3
7.00	4.96	94.0	14.5	85.5	0.24
	$t_{1/2}$(pH 6.0)/$t_{1/2}$(pH 7.0) = 10.8				

[a] Rat IgG2a (M1/42) was immobilized on a biosensor chip to a final response of 3200 RU, and solutions of wild-type or H250Q-H251N mutant FcRn were injected. At approximately 1 min into the dissociation phase, buffers (50 mM sodium phosphate, 150 mM NaCl) were injected at pH values from 6.0 to 7.0. Rate constants, % R, and $t_{1/2}$ values were calculated as described in Materials and Methods and the legend to Table 1.

To study the effects of two of the IgG histidines, we took advantage of sequence differences between different subtypes of murine IgG. Unlike most other mouse, rat, and human IgG subtypes, FcRn interface residues 433 and 435 of mIgG2b are not histidines. We therefore compared the pH dependence of the affinity of mIgG2b versus mIgG2a for FcRn. The pH dependence of the FcRn/mIgG2b interaction was indeed reduced compared to the FcRn/mIgG2a interaction, primarily due to the higher affinity of mIgG2b for FcRn at pH 7.0 (Table 1A). A Hill plot analysis (Figure 2) of the data suggests that two titrating residues on the mIgG2b/FcRn complex versus three titrating residues on the mIgG2a/FcRn complex participate in the pH-dependent affinity transition.

Analysis of the dissociation rates of FcRn/IgG complexes as a function of pH enables an estimation of the physiological lifetimes of complexes upon exposure to the neutral or slightly basic pH environment at the basolateral surface of intestinal epithelial cells. Our results indicate that FcRn/

mIgG2b complexes formed at low pH have a longer lifetime upon exposure to a pH 7.0 environment than FcRn/mIgG2a complexes (Table 1B). The diminished pH dependence of the dissociation rate of mIgG2b versus mIgG2a from FcRn reported in the present studies is likely to be due to the reduced number of histidine residues on IgG2b located at the FcRn interface. The question of whether the reduced pH dependence of mIgG2b results from the substitution of histidine 433, histidine 435, or both residues could not be evaluated in this experiment. However, using a mutant hIgG4 in which residue 435 was changed to an arginine (H435R) (Artandi *et al.*, 1992), we were able to assess the role of this residue in the pH dependence of IgG interactions with FcRn. We show that the pH dependence of the dissociation rates of H435R/FcRn complexes is unaltered comparable to wild-type hIgG4/FcRn complexes (Table 2B), suggesting that histidine 435 does not play a role in facilitating release of IgG at high pH values. Thus, the slower dissociation rate of mIgG2b from FcRn at pH 7.0 is explained if neutralization of a positive charge at residue 433 is a mechanism for decreasing the affinity of the FcRn/IgG interaction and thereby facilitating release of FcRn at higher pH values. In mIgG2b, residue 433 (lysine) is expected to maintain a positive charge over the pH 6.0−7.0 range, whereas histidine 433 in other IgGs including mIgG2a should deprotonate. The reduced pH dependence of the dissociation rates of FcRn/mIgG2b complexes compared to FcRn/mIgG2a complexes can be attributed to the lysine at position 433. Consistent with the hypothesis that a positive charge on IgG residue 433 contributes to an increased affinity for FcRn, the FcRn/Fc cocrystal structure shows negatively charged residues on FcRn (Glu 132, Glu 135, and Asp 137) in the vicinity of this IgG residue (Burmeister *et al.*, 1994a).

Analysis of FcRn binding by the 252−254 (MIS to GGG) and the 309−311 (LHQ to GGG) mutants of human IgG suggests that one or more of the residues that were altered in each of the mutants constitute a "functional epitope" in the FcRn/IgG complex, whereas alteration of residue 435 has no significant effect on the affinity (Table 2A, Figure 3). A functional epitope is defined as the residues at the contact interface between two proteins that most significantly stabilize the complex and is distinguished from a structural epitope, which constitutes all residues at the intermolecular interface (Cunningham & Wells, 1993). The reduced affinities of the 252−254 and the 309−311 mutants result primarily from slower association rates. The respective wild-type sequences of the 252−254 and the 309−311 mutants are MIS and LHQ; of these residues, only the histidine at position 310 is expected to alter its interactions over the pH range between 6.0 and 7.0, since the imidazole side chain should deprotonate over this pH range. In wild-type IgG, neutralization of the positive charge at histidine 310 as the pH is raised could result in a reduction in the association rate of the FcRn/IgG complex and a consequent reduction in the affinity. Since the pH dependence of the dissociation rate of the 309−311 hIgG4 from FcRn is reduced compared to wild-type hIgG4/FcRn or H435R/FcRn complexes (Table 2B), titration of histidine 310 may also play a role in facilitating release of IgG at high pH values. Analysis of the crystal structure of the FcRn/Fc complex predicts that Glu 117 of FcRn interacts with IgG histidine 310, supporting the hypothesis that this residue participates in the pH-dependent FcRn/IgG interaction.

We have demonstrated that a portion of the pH-dependent affinity change between FcRn and IgG can be accounted for by a collection of residues within the IgG ligand. It is noteworthy that the binding site on IgG for FcγRI, an Fc receptor that does not show pH-dependent binding to IgG, has been localized to the hinge and adjacent C_H2 domain (Duncan *et al.*, 1988; Canfield & Morrison, 1991). This region of Fc is spatially distant from the C_H2-C_H3 domain interface containing the conserved histidines implicated in this study (Figure 1A). However, several other proteins bind to IgG at the junction between the C_H2 and C_H3 domains. These include protein A (Deisenhofer, 1981), protein G (Sauer-Eriksson *et al.*, 1995), the putative Fc receptor involved in IgG catabolism (Kim *et al.*, 1994b), and RF autoantibodies (Artandi *et al.*, 1992). One or more of the conserved histidines have been shown to be contact residues in complexes of these proteins with IgG, yet the sharply pH-dependent binding profile seen for FcRn binding to IgG appears to be unique to its interaction with IgG. Differences in IgG binding by FcRn compared to the other proteins can be attributed to unique sets of interactions between each protein and IgG and to the involvement of FcRn residues not directly at the IgG binding interface (such as FcRn histidines 250 and 251).

We previously used site-directed mutagenesis to explore the possible involvement of FcRn histidine residues in the pH-dependent interaction with IgG (Raghavan *et al.*, 1994). The only FcRn heavy-chain histidines observed to affect IgG binding were a pair in the α3 domain (residues 250 and 251). Alteration of these residues to their counterparts in MHC class I molecules resulted in an FcRn molecule with about 6-fold lowered affinity for IgG at pH 6.0 (Raghavan *et al.*, 1994). The histidine pair is located at the interface of a crystallographically observed FcRn dimer of heterodimers (Burmeister *et al.*, 1994a,b) (Figure 1B), the formation of which is required for high-affinity binding of IgG (Raghavan *et al.*, 1995). Thus, titration of one or more residues of the histidine pair in wild-type FcRn could indirectly affect IgG binding affinity, by stabilizing the FcRn dimer at pH 6.0−6.5 (permissive for IgG binding) and destabilizing the FcRn dimer at pH 7.0−7.5 and above (nonpermissive for IgG binding). This hypothesis is supported by the finding that His 250 of one FcRn heavy chain interacts with Glu 89 of the β2m domain of the dimer-related FcRn molecule (Burmeister *et al.*, 1994b), suggesting that a positive charge on residue 250 should contribute to the stability of the FcRn dimer at pH 6.0. In the present study we show that the pH dependence of the dissociation rate of FcRn H250Q-H251N mutant/IgG complexes is reduced compared to wild-type FcRn/IgG complexes (Table 3); thus the pH dependence of the dissociation rates of FcRn/IgG complexes does not entirely result from titration of residues within the IgG ligand.

Our studies suggest that the sharp pH dependence of the FcRn/IgG interaction is likely to be a result of multiple events involving residues in both proteins. These events include (i) titration of FcRn/IgG interface histidine residues such as IgG residues 433 and 310 and (ii) destabilization of the crystallographically observed FcRn dimer (Burmeister *et al.*, 1994a,b) by phenomena such as the titration of FcRn histidines 250 and/or 251. Both phenomena are likely to be involved in the overall affinity transition, perhaps coupled with pH-dependent structural changes in FcRn correlating with IgG binding and release (Raghavan *et al.*, 1993). An

interesting challenge for the future lies in the construction of an FcRn/IgG complex of invariant affinity over the pH range from 6.0 to 7.5.

ACKNOWLEDGMENT

We thank Arthur Chirino for help with using Mathematica and for making Figure 1A, Dan Vaughn for suggesting the $t_{1/2}$ calculations, and Dan Vaughn and Luis Sanchez for critical reading of the manuscript.

REFERENCES

Artandi, S. E., Calame, K. L., Morrison, S. L., & Bonagura, V. R. (1992) *Proc. Natl. Acad. Sci. U.S.A. 89*, 94−98.

Burmeister, W. P., Huber, A. H., & Bjorkman, P. J. (1994a) *Nature 372*, 379−383.

Burmeister, W. P., Gastinel, L. N., Simister, N. E., Blum, M. L., & Bjorkman, P. J. (1994b) *Nature 372*, 336−343.

Canfield, S. M., & Morrison, S. L. (1991) *J. Exp. Med. 173*, 1483−1491.

Cunningham, B. C., & Wells, J. A. (1993) *J. Mol. Biol. 234*, 554−563.

Deisenhofer, J. (1981) *Biochemistry 20*, 2361−2370.

Duncan, A. R., Woof, J. M., Partridge, L. J., Burton, D. R., & Winter, G. (1988) *Nature 332*, 563−564.

Fägerstam, L. G., Frostell-Karlsson, A., Karlsson, R., Persson, B., & Rönnber, I. (1992) *J. Chromatogr. 597*, 397−410.

Gastinel, L. N., Simister, N. E., & Bjorkman, P. J. (1992) *Proc. Natl. Acad. Sci. U.S.A. 89*, 638−642.

Huber, A. H., Kelley, R. F., Gastinel, L. N., & Bjorkman, P. J. (1993) *J. Mol. Biol. 230*, 1077−1083.

Jones, E. A., & Waldman, T. A. (1972) *J. Clin. Invest. 51*, 2916.

Kabat, E. A., Wu, T. T., Perry, H. M., Gottesman, K. S., & Foeller, C. (1991) *Sequences of proteins of immunological interest*, U.S. Department of Health and Human Services, Bethesda, MD.

Kim, J.-K., Tsen, M.-F., Ghetie, V., & Ward, E. S. (1994a) *Eur. J. Immunol. 24*, 2429−2434.

Kim, J.-K., Tsen, M.-F., Ghetie, V., & Ward, E. S. (1994b) *Scand. J. Immunol. 40*, 457−465.

Kraulis, P. J. (1991) *J. Appl. Crystallogr. 24*, 946−950.

Malmqvist, M. (1993) *Nature 361*, 186−187.

Raghavan, M., Gastinel, L. N., & Bjorkman, P. J. (1993) *Biochemistry 32*, 8654−8660.

Raghavan, M., Chen, M. Y., Gastinel, L. N., & Bjorkman, P. J. (1994) *Immunity 1*, 303−315.

Raghavan, M., Wang, Y., & Bjorkman, P. J. (1995) *Proc. Natl. Acad. Sci. U.S.A. 92*, 11200−11204.

Rodewald, R. (1976) *J. Cell Biol. 71*, 666−670.

Rodewald, R., & Kraehenbuhl, J.-P. (1984) *J. Cell Biol. 99*, S159−S164.

Sauer-Eriksson, A. E., Kleywegt, G. J., Uhlen, M., & Jones, T. A. (1995) *Structure 3*, 265−278.

Simister, N. E., & Rees, A. R. (1985) *Eur. J. Immunol. 15*, 733−738.

Simister, N. E., & Mostov, K. E. (1989a) *Nature 337*, 184−187.

Simister, N. E., & Mostov, K. E. (1989b) *Cold Spring Harbor Symp. Quant. Biol. 54*, 571−580.

Tao, M.-H., & Morrison, S. L. (1989) *J. Immunol. 143*, 2595−2601.

Wallace, K. H., & Rees, A. R. (1980) *Biochem. J. 188*, 9−16.

Wolfram, S. (1991) *Mathematica, A System for Doing Mathematics by Computer*, 2nd ed., Addison-Wesley Publishing Co., Inc., Redwood City, CA.

BI951539Q